

Virtual Reality Digitization of Driving Learning Simulators: Optimization via Fuzzy Compensation

Shuai Wang¹, Bingsheng Cui^{2,*}

¹Academy of Fine Arts, Hulunbuir University, Hulunbuir 021000, China

²School of Arts and Design, Qiqihar University, Qiqihar 161000, China

Received 15 Sep 2025

Accepted 12 Feb 2026

Abstract

Virtual reality technology has significant potential in enhancing the realism and interactivity of driving simulators. However, traditional simulators often have problems such as motion perception distortion and high hardware requirements. To address the above issues, a VR digitalization method for driving simulators based on a washout algorithm optimized by fuzzy compensation is proposed. By integrating a fuzzy controller, it dynamically adjusts the filter parameters and gain weights within the framework of the washing algorithm, thereby enhancing the fidelity of motion prompts and reducing perceptual conflicts. The experimental results show that when the banquet method is subjected to an instantaneous acceleration of 1.7 G on a rough road surface, the output position error is only 12.7 mm, the acceleration accuracy reaches 99.7% under a vertical resultant force of 0.5kN, and the maximum processor occupancy rate during operation is only 58%. The above results indicate that this method not only enhances the realism of the simulation but also maintains low computational and hardware requirements, and effectively alleviates motion sickness in the simulator through adaptive motion perception adjustment.

© 2026 Jordan Journal of Mechanical and Industrial Engineering. All rights reserved

Keywords: Simulator; Fuzzy compensation; Wash-out algorithm; Filtering; Virtual Reality..

1. Introduction

With the continuous development of science and technology, Virtual Reality (VR) technology has been widely used in various fields, especially in the field of driving learning simulators. Driving learning simulator is a device that simulates the real driving environment, which can help drivers learn and train driving skills in a safe environment [1, 2]. However, traditional driving learning simulators have certain limitations, such as insufficient realism and low interactivity [3]. Currently, research on driver learning simulators mainly focuses on improving the realism, interactivity, operational efficiency and stability of the simulators. Methods to enhance the realism of simulators often require a large amount of experimental data and complex computational processes, making it difficult to achieve a balance between real-time performance and simulation accuracy [4]. Secondly, methods to enhance simulator interactivity are often limited by the development level of hardware devices and software platforms, making it difficult to meet the needs of different users. In addition, methods to optimize the performance of simulators often require large changes to the structure of the simulator, increasing the complexity and difficulty of the research [5]. Washout algorithms can effectively process simulator data and improve the realism and interactivity of the simulator.

VR technology can provide drivers with a more realistic and immersive simulated driving experience, enhancing their sense of engagement and learning. Although the washing algorithm in the current research can effectively handle low-frequency motion perception signals, it is vulnerable to the nonlinear fluctuations of the input signal in dynamic scenes, resulting in platform reset delay and perception distortion. Fuzzy compensation technology can optimize the nonlinear response characteristics of the algorithm in real time by dynamically adjusting the filtering parameters and gain weights.

Therefore, combining fuzzy compensation with the washing algorithm can not only retain the physical modeling ability of the washing algorithm for acceleration perception, but also solve the control conflicts under complex inputs through fuzzy reasoning, thereby improving the authenticity of the simulator signal while ensuring real-time performance. In this context, the study tries to propose a VR digitalization technique for driving learning simulators by combining VR technology with simulators, and innovatively adds a fuzzy compensation optimized wash-out algorithm to the technique for data processing. The current research problem is that traditional washout algorithms use fixed parameter filters, which are difficult to adapt to the dynamic requirements of multiple scenarios and driving modes, and can easily cause platform saturation or distortion of motion prompts. At the same time, there is a delay or spectral mismatch between the motion platform prompt and visual/vestibular perception,

* Corresponding author e-mail: 18047071182@163.com.

which exacerbates sensory conflicts and leads to simulator motion sickness in users, affecting training effectiveness and user experience.

The research is mainly conducted in four parts, the first part discusses and summarizes the current research results related to driving simulators and wash-out algorithms. The second part focuses on the design of VR digitalization technology for driving learning simulator based on fuzzy compensation optimization of wash-out algorithm. The third part is the performance test and application analysis of the research method. The last part is to discuss and summarize the whole paper.

In the research, the technological innovation of the driving learning simulator is mainly reflected in its unique VR digital technology and the combination of fuzzy compensation optimization and elimination algorithms. The innovation of the research method is reflected in the construction of the motion perception model through the washing algorithm, combined with the parameters of the fuzzy compensation dynamic optimization algorithm, to form a closed-loop control mechanism. This design not only inherits the biological perception simulation advantages of the washout algorithm, but also compensates for its insufficient robustness in dynamic scenes through fuzzy compensation. The washing algorithm is responsible for simulating the acceleration perception threshold of the human vestibular system, while the fuzzy controller adjusts the cut-off frequency and damping ratio of the high/low pass filter in real time based on the nonlinear characteristics of the input signal, thereby reducing the interference of the mechanical limit constraints of the platform on motion restoration. The contribution of the research lies in proposing a novel VR digital technology that combines wash-out algorithms and fuzzy control methods, providing new technical references for the field of driving learning. This study aims to address the conflict between high realism and low hardware resource consumption in current driving simulators for motion prompt restoration, and provide strong guidance for the design and application of future driving simulators to better adapt to the needs of different users.

2. RELATED WORKS

2.1. Virtual Reality Technology Applications

With the increase of car ownership, more scholars realize the importance of car driving learning simulators. Some scholars have conducted related research on driving simulators. Azevedo-Sa and other scholars [6] proposed a method based on trust measurement for the problem of automatic driving in driving simulators. The process uses Kalman filtering to integrate the driver behavior and investigate the factors affecting the trust of the system. The experimental results show that the proposed method can effectively improve the simulation quality. Zhai et al. [7] proposed a technique incorporating the queuing effect for the problem of driving simulation in Internet vehicles. The process uses a kinematic shockwave model to predict the queue length for the vehicle saturation case, and splits the optimization problem to optimize the trajectory. The experimental results show that the proposed method can effectively improve the vehicle control performance. Liu et al. [8] proposed a data-driven approach based on driving simulation for the driving simulation problem in transportation systems. The process uses data-driven simulation to define the coordination sub-module of the

transportation system, and introduces long and short-term memory networks to construct a prediction framework. The experimental results show that the proposed method can perform accurate driving simulation. Miri et al. [9] proposed a method based on energy modeling for the problem of driving simulation in electric vehicles. The process models the vehicle dynamics and powertrain, and analyzes the vehicle control efficiency taking into account the driver behavior. The experimental results show that the proposed method has good simulation accuracy. Ding et al. [10] proposed a method with time as the main information for the lane changing path problem in automatic driving simulation. The process uses lane change time and vehicle longitudinal displacement to calculate the trajectory. Experimental results show that the proposed method can effectively improve the quality of driving simulation.

2.2. Algorithms for Car Driving Learning Simulators

There are also scholars who have conducted research on simulators designed by VR technology. Wu et al. [11] used the driving simulator of 360° panoramic video combined with VR technology to study the influence of takeover auxiliary information of different types of augmented reality head-up display on the driver's situational awareness. The results show that the augmented reality head-up display of situational awareness can best improve the driver's situational awareness and takeover performance. Zeuwts et al. [12] used VR technology to assess the hazard detection and prediction abilities of child cyclists through headsets and virtual environment simulators. The study verified the effectiveness of VR simulators by recording riding speed, braking reaction and eye movement data. The results show that the obvious danger situation is easier to be watched and brake in advance than the hidden danger situation, which verifies the content validity of the simulator. Zhang et al. [13] designed and developed an exploration-based educational VR game for the Apollo lunar rover mission. The game provides an immersive experience, with content presented in an exploratory play style, and players can choose between active or passive learning modes, learning space, facts and operational knowledge. User research shows that VR technology can effectively improve learning effect and participation, and discusses the influence of different learning modes on learning outcomes, providing teaching enlightenment for the development of educational VR games of similar historical events.

Some other scholars have conducted related research on washout algorithms. Houda and other scholars proposed a method based on washout algorithms to address the Handiski simulator performance problem. The process uses an 8-degree-of-freedom mechatronics platform as a physical carrier and a motion cueing algorithm to respond to the mid-frequency range information. The experimental results show that the proposed method can effectively improve the simulation realism [14]. Duc-An et al. propose a method based on the motion cueing algorithm for the design problem of multi-sensory systems. The algorithm is optimized by using proprioceptive model in the process. The experimental results show that the proposed method has good accuracy [15]. Kalyanaraman et al. propose a method of fusion wash-out algorithm for the construction of coupled model of railroad ballast washout. The process provides a unified representation of regions with nonlinear permeability and uses advection equations to control porosity. Experimental results show that the proposed

method has good numerical accuracy [16]. Qazani et al. proposed a method based on wash-out algorithm for the problem of urban traffic simulation. The process uses a penalty function to limit the displacement of the moving platform. The experimental results show that the proposed method is effective for traffic simulation [17]. Dasu et al. proposed a method incorporating washout algorithm for power system signal enhancement. The process uses a combination of multi-computer system and single-computer infinity system, and utilizes the objective function of eigenvalues for stabilizer design. Experimental results show that the proposed method has good test accuracy [18].

In summary, although the wash-out algorithm has been studied or applied in many fields, there is a lack of research on automotive driving learning simulators. In view of this, the study tries to design the driving learning simulator based on the wash-out algorithm and make innovative improvements using other technologies, in order to provide certain technical references for the simulator design.

3. DESIGN OF VR DIGITAL TECHNOLOGY FOR DRIVING LEARNING SIMULATOR

Driving simulators provide a safe and risk-free environment for learners to practice their driving skills. This section elaborates on the technological tools used in the VR digitalization of the research-designed driving learning simulator.

3.1. Design of Simulation Algorithm for Simulator Based on Washout Algorithm

In the current technological environment, many race car athletes, truck drivers and even civilian car drivers have started to use VR digital learning to drive simulators for driving practice in order to improve their driving skills [19, 20]. The simulator's ability to reproduce signals and adjust parameters during operation determines the simulation quality [21]. The washout algorithm, which simulates acceleration through human motion perception, can effectively improve the signal reproduction ability. Based on the washout algorithm, a VR driving learning simulator is designed. Firstly, the motion model of the driving learning simulator is designed, as shown in Fig. 1.

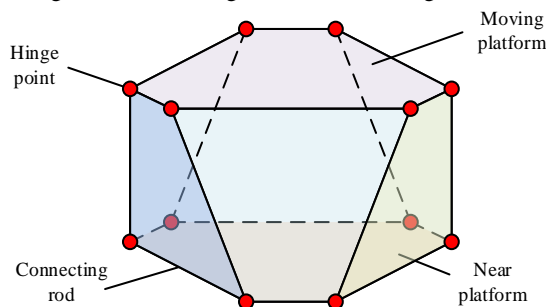


Figure 1. Simulator motion model

As seen in Fig. 1, the motion model of the driver learning simulator is mainly composed of connecting rods and hinge points. In the motion model, there are two surfaces parallel to each other in the initial position, both surfaces are hexagonal, surrounded by six hinge points and six connecting rod connections. The face in the high position serves as the movable kinetic platform and the face in the low position serves as the immovable static platform. When the electric cylinder performs coordinated extension

and retraction, the moving platform can generate rotational movements such as pitch, roll, and yaw, as well as multi-axial translation, simulating the dynamics of vehicle acceleration, braking, and steering, and giving the human body a sense of movement and rotation. The human body uses the vestibular system and visual information to acquire motion states, where the vestibular system is mainly composed of otoliths and semicircular canals for contrasting force, acceleration and rotation [22]. The simulator can perform reset operations to realize long commands through the sensory thresholds of the vestibular system. Specifically, the angular acceleration threshold (approximately $0.5^\circ/s^2$) is derived from vestibular perception research and is commonly used in the design of motion suggestion algorithms; the threshold for linear acceleration (approximately 0.08 m/s^2) is based on vestibular physiology. The reset mechanism refers to the inability of users to perceive sustained motion when the platform motion is below the above threshold, so the platform can gradually reset without causing dizziness, extending the effective motion space. The transfer function of rotation information in the semicircular canal is shown in Equation (1).

$$\frac{\hat{\omega}}{\omega} = \frac{\tau_a s}{(\tau_a s + 1)} \cdot \frac{\tau_1 s}{(\tau_1 s + 1)(\tau_2 s + 1)} \quad (1)$$

In Equation (1), $\hat{\omega}$ represents the angular velocity perceived by the simulator's semicircular canal; ω represents the vestibular angular velocity input to the simulator's semicircular canal; τ_a represents the semicircular canal adaptation time constant; s represents Laplace variable; τ_1 represents the semicircular canal long time constant; and τ_2 represents the semicircular canal short time constant. The short time constant characterizes the fast response dominated by mechanical inertia and describes the initial flow stage of endolymph in the semicircular canals, which is determined by both fluid inertia and pipeline elasticity; The long-term constant characterizes the dynamic equilibrium dominated by viscous damping, describes the attenuation process of lymphatic flow, adapts to the slow tuning of neural signals, and describes the electrochemical adaptation process of hair cells and vestibular nerves. Due to the capture of core features such as high pass and band-pass characteristics caused by adaptation in vestibular perception, virtual driving motion perception can be achieved. Therefore, the study only uses a vestibular system model for description, where the transfer function in the semicircular canals is used to guide the design of the washing out algorithm's rotation channels (yaw, pitch, roll) to ensure that the simulated angular motion remains within a reasonable perceptual bandwidth. The transfer function in the otolith provides a basis for the design of translation and tilt coordination channels, ensuring that low-frequency linear acceleration cues can be appropriately simulated through platform tilt (gravity illusion) while minimizing error cues. The two together form the perceptual basis for adjusting the filter parameters of the washout algorithm. The transfer function of specific motion in otolith is shown in Equation (2).

$$\frac{\hat{f}}{f} = \frac{K(1 + \tau_a s)}{(\tau_L s + 1)(\tau_s + 1)} \quad (2)$$

In Equation (2), \hat{f} represents the angular velocity perceived by the simulator's otolith; f represents the vestibular angular velocity input to the simulator's otolith; K represents the otolith input index; τ_a represents the otolith adaptation time constant; τ_s represents the otolith long time constant; and τ_L represents the otolith short time constant. The transfer functions described by Equation (1) and Equation (2) are not a complete physical model of the entire system, but are simplified linear transfer functions used to represent angular velocity perception and motion in the otolith. Equation (1) simulates human rotation perception through the angular velocity transfer characteristics of semicircular canals, which is used to calibrate the biological rationality of dynamic responses such as platform yaw and pitch in the washing algorithm. Equation (2) establishes the perception logic of the vestibular system for braking and acceleration based on the linear acceleration transfer model of otoliths, guiding the design of filter parameters to suppress low-frequency drift and match the human perception threshold. The two together constitute the physiological basis of the motion control algorithm. The structure of the constructed washout algorithm is shown in Fig. 2.

As seen in Fig. 2, the wash-out algorithm in the driving simulator mainly consists of three filtering operations. Both semicircular and otolith input information need to be scale-restricted first. After the otolith information is proportionally limited, a part of it performs Eulerian angular velocity transform and combines with the gravity information to perform high-pass filtering operation, and then integrates twice to output the distance signal. The other part performs low-pass filtering, tilt coordination, and angular velocity limiting before combining with the semicircular information. The semicircular information is scaled and limited and then transformed to Eulerian angle and velocity, and then high pass filtering operation is performed to transform to Eulerian angle. Motion control of the simulator is achieved by angular and distance signals. The absolute acceleration information collected by the simulator vestibule is shown in Equation (3).

$$\bar{a}_A = \frac{d\bar{v}_0}{dt} + \frac{d\bar{w}}{dt} \times \bar{r}_A + \bar{w} \times (\bar{w} \times \bar{r}_A) \quad (3)$$

In Equation (3), \bar{a}_A represents the absolute acceleration information collected by the simulator's vestibule; \bar{v}_0 represents the coordinate system center-of-mass velocity; \bar{w} represents the non-center-of-mass angular velocity; and \bar{r}_A represents the position vector of the simulator's head. Equation (3) describes the absolute acceleration information of the simulator, which is collected by the simulator's motion platform. The calculation takes into account the velocity of the center of the coordinate system, the angular velocity of the non-center and the relative position vector of the simulator head. The acceleration information can be calculated by the control algorithm or realized by the actual hardware response of the simulator. If calculated, this acceleration information is often used during the design process to adjust the response of the motion platform to ensure that the simulator can accurately reproduce different driving scenarios. The specific force information received by the simulator is calculated as shown in Equation (4).

$$\bar{f}_{AA} = \bar{a}_A - \bar{g}_A \quad (4)$$

In Equation (4), \bar{f}_{AA} represents the specific force information; \bar{g}_A represents the gravity vector. The transfer function of the high pass filter is shown in Equation (5).

$$H_{ah}(s) = \frac{K_a s^3}{(s^2 + 2\xi_{ah}\omega_{ah}s + \omega_{ah}^2)(s + \omega_a)} \quad (5)$$

In Equation (5), $H_{ah}(s)$ represents the high-pass filter transfer function; K_a represents the high-pass proportionality coefficient; ξ_{ah} represents the high-pass filter acceleration filter damping ratio; ω_a represents the first-order frequency response value; and ω_{ah} represents the high-pass filter acceleration filter cutoff frequency. The second-order filter is used to construct the low-pass filter acceleration channel, and the transfer function is shown in Equation (6).

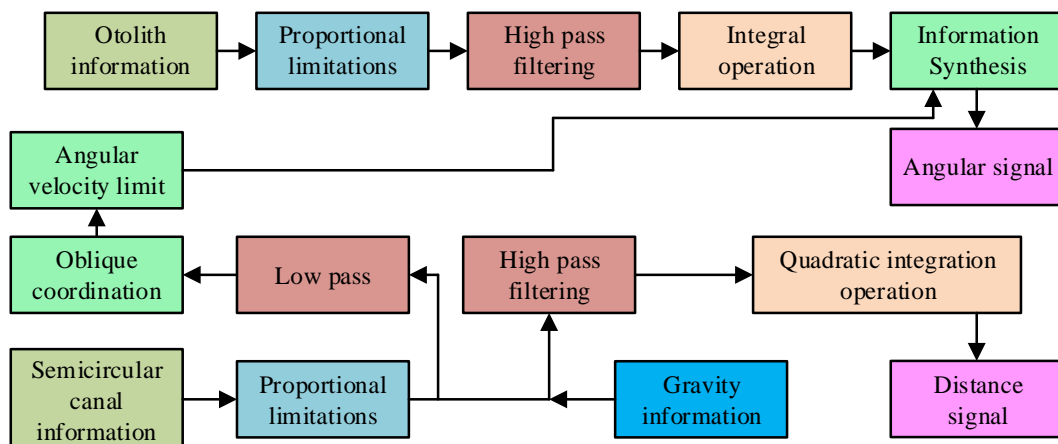


Figure 2. Washout algorithm structure

$$H_{al}(s) = \frac{K_c \omega_{al}^2}{s^2 + 2\xi_{al} \omega_{al} s + \omega_{al}^2} \quad (6)$$

In Equation (6), $H_{al}(s)$ represents the low-pass filter acceleration channel transfer function; K_c represents the low-pass scaling factor; ω_{al} represents the low-pass filter acceleration filter cutoff frequency; ξ_{al} represents the low-pass filter acceleration filter damping rate. The high-pass and low-pass filters in Equation (5) and (6) are used as part of the washout algorithm to filter out high-frequency noise and low-frequency drift in the input signal to ensure that the simulator can accurately reproduce motion perception during driving. The parameter selection of the filter is based on the perceptual characteristics of the vestibular system and the physical limitations of the movement platform. Specifically, the cut-off frequency of the high-pass filter is calibrated experimentally, and the sensitive frequency band of human vestibular in the range of 0.1-2 Hz is preferentially reserved to match the driver's perception threshold of instantaneous acceleration. The cut-off frequency of the low-pass filter is dynamically adjusted according to the maximum displacement capacity of the moving platform to ensure that the movement of the platform does not exceed the mechanical limit.

3.2. Design of VR Digital Technology Based on Fuzzy Compensation Optimization

In the actual operating environment of driving learning simulators, the input data is highly random, which may cause control conflicts when performing simulator control. Fuzzy compensation has strong parameter applicability and has good performance in assisting simulator control [23]. The study uses fuzzy compensation to optimize the design of the simulation technique of a driver learning simulator based on wash-out algorithm. The fuzzy compensation is realized using a fuzzy controller and the structure of the fuzzy controller is shown in Fig. 3.

As seen in Fig. 3, the fuzzy controller is involved by the knowledge base in the whole process of fuzzy processing for description and processing operations. After the exact data input, the input data is first transformed by the fuzzification interface using mapping relations to generate fuzzy sets. After that, fuzzy inference is performed by fuzzy inference machine to generate fuzzy output signal. The fuzzy output signal is then fed into the defuzzification interface and processed to obtain the precise control information output.

The fuzzy controller receives two types of input signals: The first type is the displacement error of the translation channel, which characterizes the deviation of the actual displacement of the moving platform in the X, Y, and Z axis directions from the target value. The second category is the Angle error of the inclined coordination channel, reflecting the differences between the pitch Angle, roll Angle and yaw Angle of the moving platform and the expected Angle. The state variables of the system are jointly defined by the real-time translational displacement of the moving platform in three-dimensional space and its rotation angles around each axis. These state variables are fed back to the controller in real time through high-precision sensors. The output of the controller includes the dynamic correction parameters of the cut-off frequency and damping ratio of the high and low pass filters, as well as the nonlinear compensation gain coefficients of the tilt coordination channel and the high-frequency acceleration channel. The general form of fuzzy is represented using the affiliation function as shown in Equation (7).

$$\mu_A(x) = \begin{cases} 1 & x \in A \\ (0,1) & \text{part of } x \text{ belong to } A \\ 0 & x \notin A \end{cases} \quad (7)$$

In Equation (7), $\mu_A(x)$ represents the affiliation degree of the element; A represents the fuzzy set. After completing the definition of fuzzy subsets, the controller affiliation function is constructed in a refined way using triangular, Z-shaped and trapezoidal affiliation functions. The affiliation functions of the fuzzy controller with different inputs and compensation are shown in Fig. 4.

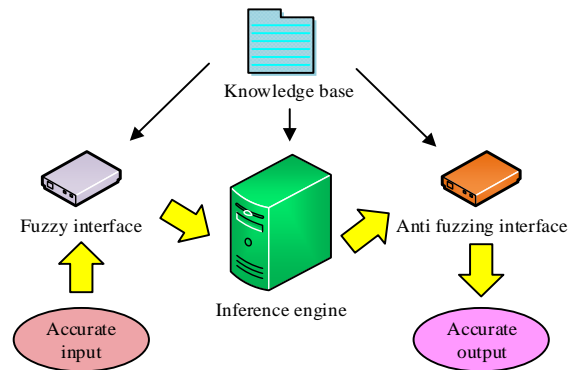


Figure 3. Fuzzy controller structure

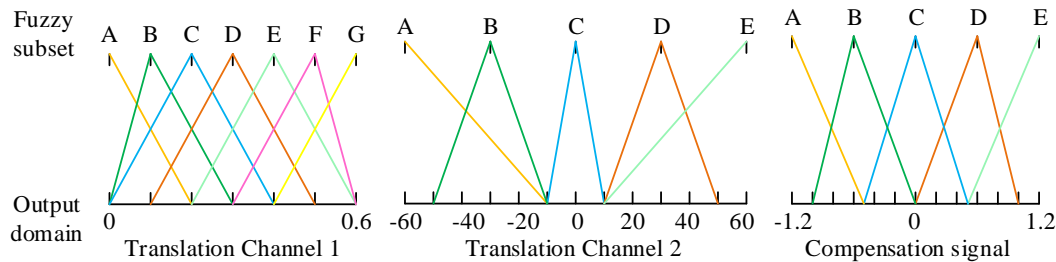


Figure 4. Fuzzy controller membership function

As seen in Fig. 4, the study sets the fuzzy subsets of the inputs and limits the domain of the outputs. The input of the fuzzy controller includes two types of signals: translation channel and tilt coordination channel, with units of mm and ° respectively; The domain of discussion is dimensionless. In the case where the fuzzy controller input is the translation channel No. 1, the fuzzy subset contains 7 input elements and the output thesis domain is [0, 0.6]. In case the fuzzy controller input is the tilt coordination channel No. 2, the fuzzy subset contains 5 input elements and the output domain is [-60, 60]. The fuzzy compensated signal input subset contains 5 input elements and the output domain is [-1.2, 1.2]. The fuzzy implication relation is calculated as shown in Equation (8).

$$\mu_{\bar{R}_M}(x, y) = \mu_{\bar{A}}(x) \wedge \mu_{\bar{B}}(y) \tag{8}$$

In Equation (8), $\mu_{\bar{R}_M}(x, y)$ represents the fuzzy implication relation; $\mu_{\bar{A}}(x)$ represents the current state fuzzy set of the system; $\mu_{\bar{B}}(y)$ represents the output state fuzzy set of the fuzzy controller; and \wedge represents the Cartesian product operation. After that the maximum affiliation method is used for the exact output of the simulator control quantities. The structure of the fuzzy compensation optimization based wash-out algorithm for driving learning simulator is shown in Fig. 5.

As can be seen in Fig. 5, the wash-out algorithm incorporating the fuzzy controller is used by the fuzzy controller for the generation of the fuzzy compensation

model. The compensation operation for the tilt coordination channel and the high frequency acceleration channel is realized by the compensation signal. The line acceleration signal is compensated after being filtered by a high-pass filter, and the signal after completing the compensation is integrated twice to obtain the translational displacement data of the simulator. The angular acceleration signal is superimposed on the compensated line acceleration signal to obtain the rotational angular shift data. By dynamically adjusting the gain weights of tilt coordination channel and high frequency acceleration channel in washout algorithm, fuzzy compensation adaptively adjusts the nonlinear input signal. Specifically, when the instantaneous G-force or acceleration changes, the fuzzy controller adjusts the damping ratio of the low-pass filter to the proportional coefficient of the high-pass filter in real time based on the membership function of the input signal (such as the "high error" of the translational channel or the "low frequency oscillation" state of the inclined channel). For example, under rough pavement conditions, the fuzzy rule base preferentially suppressed the low-frequency oscillation component of the inclined coordination channel, while increasing the gain of the high-frequency acceleration channel, thereby reducing the platform reset delay. The process of implementing the VR digitization technology of the research-designed driving learning simulator is shown in Fig. 6.

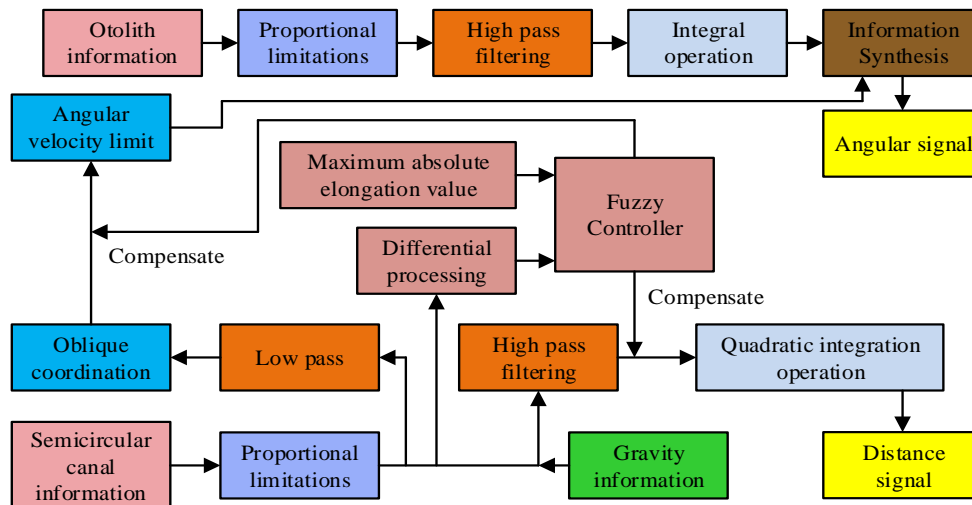


Figure 5. The washout algorithm structure of driving learning simulator based on fuzzy compensation optimization

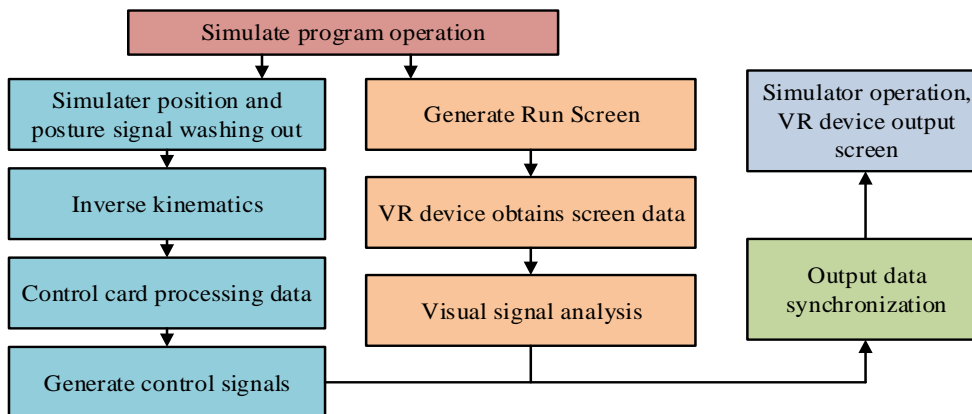


Figure 6. Implementation process of VR digital technology for driving learning simulator

As can be seen in Fig. 6, the research design driving learning simulator generates source data from the simulation program to control the simulator and the VR device at runtime. The source data, when transmitted to the simulator, first undergoes washout of simulator position and pose signals, followed by kinematic inverse solution. The control signals to the simulator are output after data processing by the control card. When the source data is transmitted to the VR device, the running screen is generated by the simulation program, and the VR device performs visual signal parsing after acquiring the screen data. After synchronizing the data of the VR device and the simulator, the action is realized by the simulator and the VR device outputs the screen to the simulator. When performing the command resolution of the washed out signals, a digital filter transformation is performed using the bilinear transformation method. The imaginary axis tangent transformation between different planes is shown in Equation (9).

$$\Omega = \frac{2}{T} \tan\left(\frac{\Omega_1 T}{2}\right) \quad (9)$$

In Equation (9), Ω represents the current plane imaginary axis; Ω_1 represents the next plane imaginary axis; T represents the sampling interval. The transformation relation is extended and carried out to the complete plane as shown in Equation (10).

$$s = \frac{2}{T} \cdot \frac{1 - e^{-s_1 T}}{1 + e^{-s_1 T}} \quad (10)$$

The single-valued mapping between surfaces with corresponding single-valued relations that eliminate spectral aliasing is shown in Equation (11).

$$z_d = \frac{\frac{2}{T} + s_d}{\frac{2}{T} - s_d} \quad (11)$$

In Equation (11), z_d and s_d represent different faces. The parameter relationships in the different order filters are analyzed and then the difference equations are derived as shown in Equation (12).

$$y(n) = 0.502x(n) - 1.507x(n-1) + 1.057x(n-2) - 0.502x(n-3) + 1.824y(n-1) - 1.027y(n-2) + 0.117y(n-3) \quad (12)$$

In Equation (12), $y(\cdot)$ represents the value of differential equation, represents the control instructions that have been optimized through the washing algorithm and fuzzy compensation; $x(\cdot)$ represents the input value, represents and characterizes the original motion parameters collected by the sensor. Discrete filters undertake key signal processing functions in driving simulators and are designed to balance hardware limitations and perception requirements. The filter enhances the system performance through three core mechanisms. High-frequency noise suppression is achieved through the low-pass characteristic. When the simulator reproduces rough roads or emergency braking, the high-frequency noise generated by the mechanical vibration of the electric cylinder is effectively attenuated. For example, in the scene of bumpy roads, the negative coefficient of the weighted historical input weakens the high-frequency resonant component, driving the electric cylinder to generate smooth motion instructions, which not only restores the real bumpy feeling but also avoids the resonance damage of the mechanical structure.

Low-frequency drift elimination relies on high-pass characteristics to separate cumulative displacement errors below 0.1Hz, ensuring that the moving platform continuously outputs acceleration signals within a limited stroke. In the continuous curve simulation, the platform resets the displacement deviation through the repositioning operation to maintain the continuity of the driving scene. Perceptual delay optimization is achieved by dynamically adjusting the damping ratio of the filter to match the physiological delay threshold of the human vestibule. The motion of the motorized cylinder is calculated after solving for position and pose as shown in Equation (13).

$$\Delta l = l_i - l_o \quad (13)$$

In Equation (13), Δl represents the amount of motorized cylinder movement; l_i represents the target length of the motorized cylinder; l_o represents the original length of the motorized cylinder. Each electric cylinder completes the movement to realize the overall position and posture change of the simulator. Since the driving simulation does not involve large spatial movements, a wired connection is used to connect the VR device, the simulator, and the computer running the simulation software to reduce the signal transmission delay.

In the process of fuzzy compensation, the creation of the knowledge base begins with the collection of multi-source data, covering physical parameters such as acceleration, angular velocity, and steering wheel Angle under typical working conditions in real vehicle tests, and combines the physiological signals of the driver for scene classification. The knowledge base adopts a hierarchical architecture design. The top layer is a standardized scene library, the middle layer stores 256 fuzzy control rules, and the bottom layer records the historically optimized filter parameter combinations. Control rules are generated through the combination of expert experience and reinforcement learning. Each rule consists of preconditions and implementation strategies. In real-time control, the fuzzy controller achieves knowledge-driven optimization through three stages: Firstly, it matches the current sensor data with the characteristics of the scene library and activates the corresponding rule set; Secondly, multi-rule reasoning is carried out based on the fuzzy implication relationship to dynamically adjust the cut-off frequency and damping ratio of the filter. Finally, the underlying parameter library is iteratively updated based on the feedback of output stability.

In the whole technology, the Wash-out algorithm effectively simulates the change of acceleration signal through high-low pass filtering and other technologies, which is mainly responsible for eliminating low-frequency noise and maintaining true motion perception. The fuzzy compensation is further optimized on the basis of the wash-out algorithm. Especially when the instantaneous G-force or acceleration changes dramatically, the fuzzy compensation can adjust the filter parameters in the algorithm in real time to reduce the delay of the moving platform and ensure that the simulator can respond quickly to changes.

In addition, the fuzzy system proposed in this study is not intended for estimating the motion characteristics of vehicles, as these characteristics are already provided as known inputs by high fidelity simulation software. On the contrary, the function of the fuzzy rule library is to serve as an adaptive optimizer for washing out the internal parameters of the algorithm. The purpose is to dynamically adjust filtering coefficients such as cutoff frequency, damping ratio, and gain weight based on the real-time status

of the motion platform, thereby enhancing the realism of motion prompts and preventing platform actuator saturation. The selection of fuzzy rules is based on the analysis of the kinematic constraints of the motion platform and the established principles of motion prompts. The core design logic is as follows: Rule principle 1: If the translation displacement error is large, slightly increase the gain of the high pass filter. This enables the platform to better reproduce high-frequency acceleration and reduce position errors by utilizing its limited travel. Rule principle 2: If the tilt coordination angle error is large, slightly reduce the damping ratio of the low-pass filter. This allows for more agile tilt response to simulate sustained low-frequency acceleration, improving perceptual matching. The membership functions for input and output were initially defined based on the physical limits of the Motus MTC-6E3000 platform, and then fine tuned through iterative simulations to find a balance between performance and stability.

4. ANALYSIS AND RESULTS OF VR DIGITAL TECHNOLOGY FOR DRIVING LEARNING SIMULATOR BASED ON FUZZY COMPENSATION OPTIMIZATION AND WASHOUT ALGORITHM

Driving simulators can simulate a variety of complex road conditions and emergencies and help learners learn to cope with these situations in a safe environment. This section will analyze the effectiveness of the VR digital technology of the research-designed driving learning simulator from the perspective of performance testing and effectiveness analysis.

4.1. Results of Performance Testing of VR Digital Technology

In order to test the performance of the research-designed driver learning simulator VR digital technology in conducting simulated driver learning for simulators, the research used Richard Burns Rally software to conduct performance simulation tests. Two types of roads, paved and rough, were used to conduct the tests. The research method

involves identification and data interaction through the driver software of the Tumast driving simulator. The operation instructions from the driver software can be directly collected within the Richard Burns Rally software. The abbreviated research method is Fuzzy compensation method (FCM), which is compared with the nonlinear deflation method [24] and acceleration somatosensory simulation method [25]. The nonlinear deflation method ADAPTS to the physical limitations of different acceleration stages by dynamically scaling the output signal of the motion platform. The core of it is to compress the signal amplitude in the high acceleration stage to avoid the platform overlimit. Compared with the research methods, it relies more on the fixed threshold adjustment strategy. The acceleration somatosensory simulation method generates motion instructions based on the feedback of the acceleration sensor and predefined filtering algorithms, and suppresses high-frequency noise through a low-pass filter with a fixed cut-off frequency. The reason for choosing the above method for comparative experiments is that the former represents the mainstream solution of handling platform physical limitations through pre-set static rules, and the core is to conservatively scale motion instructions while ensuring system security; The latter is a typical traditional method that relies on offline optimization of fixed parameter vestibular models. The process of processing raw data into performance indicators involves multiple steps. Firstly, the collected raw data is filtered to remove noise and interference. High pass and low-pass filters are used here to ensure the accuracy of the data. Secondly, by implementing mathematical model calculations on the processed data, the final performance indicators are obtained. The study measures position error by comparing the absolute distance between the actual position of the simulator motion platform and the theoretical standard position. High precision laser rangefinder sensors were used to collect position data. Specifically, the laser rangefinder can provide real-time feedback on the platform's position changes, ensuring high accuracy. Firstly, the position error of the output simulator position is compared, and the absolute distance between the center point of the moving platform and the center point of the theoretical standard is measured, as shown in Fig. 7.

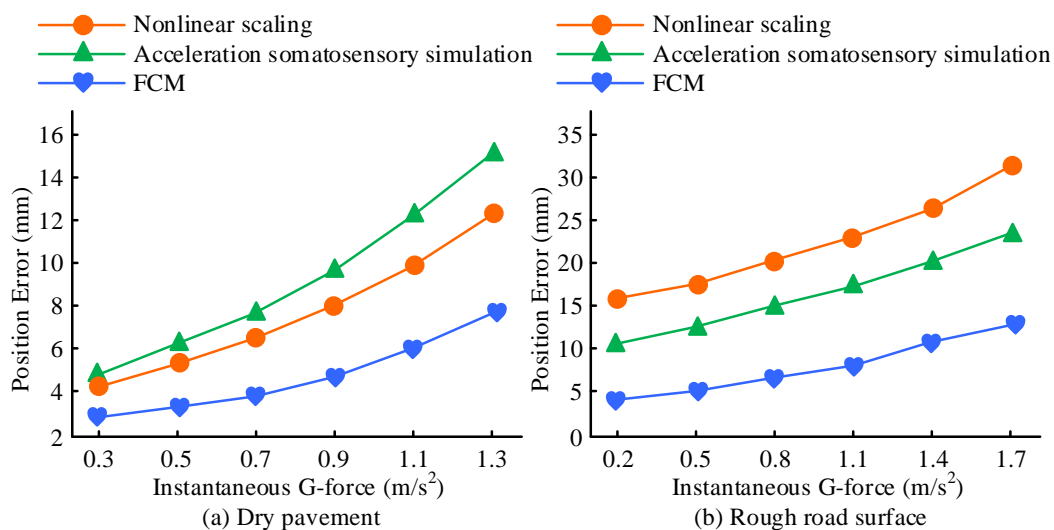


Figure 7. Output position error

As seen in Fig. 7, the output position errors of the different methods all increase with the rise of the instantaneous G force theoretically applied to the simulator. As shown in Fig. 7(a), in the paved road, the output position error of the nonlinear deflation method reaches 12.3 mm when the instantaneous G force reaches 1.3, and that of the acceleration somatosensory simulation method reaches 15.0 mm. the output position error of the FCM is 2.9 mm when the instantaneous G force reaches 0.3, and that of the FCM is 7.7 mm when the instantaneous G force reaches 1.3. As shown in Fig. 7(b), in the rough road, the output position error of the different methods increases with the increase of the theoretical G force on the simulator.), the output position error of the nonlinear deflation method reaches 31.7 mm when the instantaneous G force reaches 1.7, and the output position error of the acceleration body sensing simulation method reaches 23.5 mm for the FCM, which has a better output position accuracy when the instantaneous G force reaches 0.2, and the output position error of 12.7 mm when the instantaneous G force reaches 1.7 which has a better output position accuracy. The evaluation of acceleration accuracy is based on vertical acceleration data collected through MEMS accelerometer acceleration sensors. Sensors are installed on the motion platform of the simulator, which can monitor acceleration changes in real time and transmit data to the computing system for analysis. Test the accuracy of the acceleration output by the simulator, select the vertical acceleration of the simulator as the test data, and compare it with the latest Digital Technology and Digital Technologies in Logistics 4.0 [26-28]. The comparison of acceleration accuracy is shown in Fig. 8.

As shown in Fig. 8, the acceleration accuracy of each method decreases as the vertical resultant force increases. As shown in Fig. 8 (a), when the vertical resultant force reaches 2.5kN on the paved road surface, the acceleration accuracy of Digital Technology decreases to 98.3%; The acceleration accuracy of Digital Technologies in Logistics 4.0 has decreased to 97.8%. When the vertical resultant force is 0.5kN, the acceleration accuracy of FCM is 99.7%; When the vertical resultant force reaches 2.5kN, the accuracy of acceleration decreases to 99.5%. As shown in Fig. 8 (b), on rough road surfaces, when the vertical resultant force reaches 2.5kN, the acceleration accuracy of Digital Technology decreases to 98.1%; The acceleration accuracy of Digital Technologies in Logistics 4.0 has decreased to 98.0%. When the vertical resultant force is 0.5kN, the acceleration accuracy of FCM is 99.5%; When the vertical resultant force reaches 2.5kN, the accuracy of acceleration decreases to 99.1%. This indicates that the research method has better acceleration simulation accuracy.

4.2. Application Analysis of VR Digital Technology in Driving Learning Simulator

For the application analysis of the VR digital technology of the research-designed driving learning simulator, the simulator was built using Motus MTC-6E3000 six-degree-of-freedom platform as the motion platform. Tumast T300 was used as the driving operation simulator. HTC VIVE Pro 2 is used as the VR visual communication device. The experimental setup used is shown in Fig. 9.

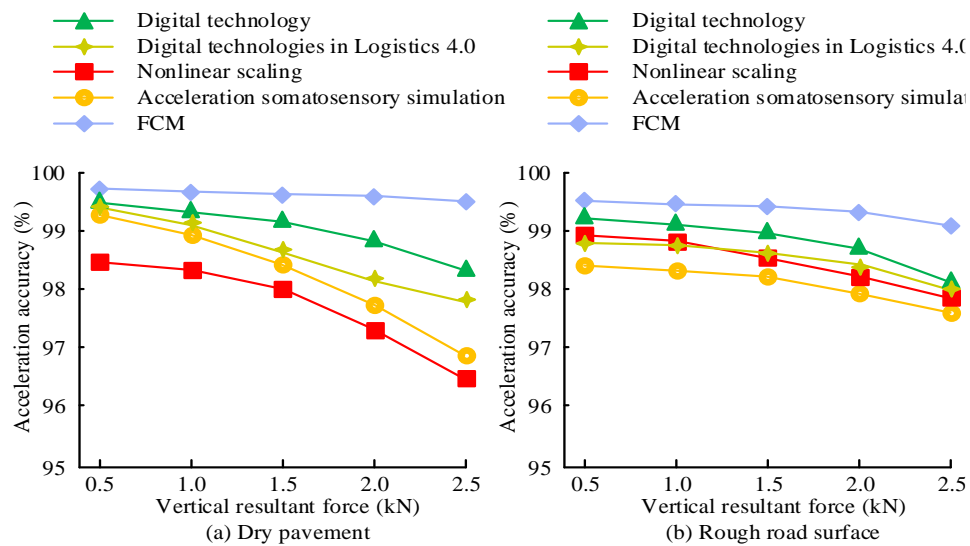


Figure 8. Acceleration accuracy

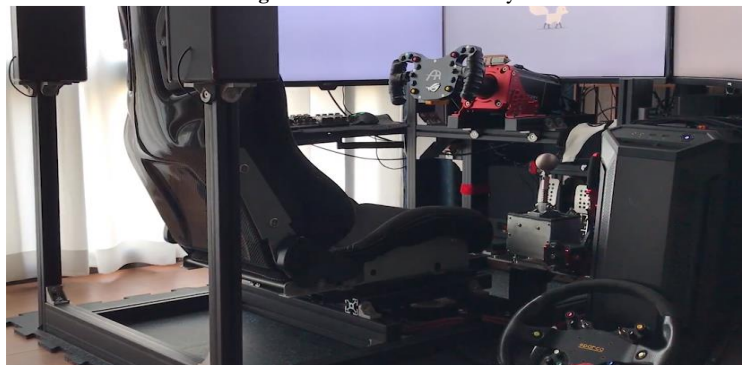


Figure 9. Experimental setup

Dirt Rally 2.0 was used as the application analysis software, and the Rallye Automobile Monte-Carlo scenario was used as the paved road scenario and the Finland scenario was used as the rough road scenario. The computer processor for the analysis is i7-13400H and the graphics card is RTX-4070Ti. The response latency of the device is analyzed as shown in Fig. 10.

As seen in Fig. 10, the device operation response delay of different methods fluctuates within a certain interval. As shown in Fig. 10 (a), the device response latency of FCM

fluctuates between 1.3ms and 8.9ms, with an average response delay of 5.3ms. As shown in Fig. 10 (b), the device response latency of Nonlinear scaling fluctuates between 2.4ms and 15.7ms, with an average response delay of 9.6ms. As shown in Fig. 10 (c), the device response latency of the Acceleration soybean simulation fluctuates between 4.9ms and 19.8ms, with an average response latency of 12.1ms. The processor occupancy when the simulator is running is analyzed, as shown in Fig. 11.

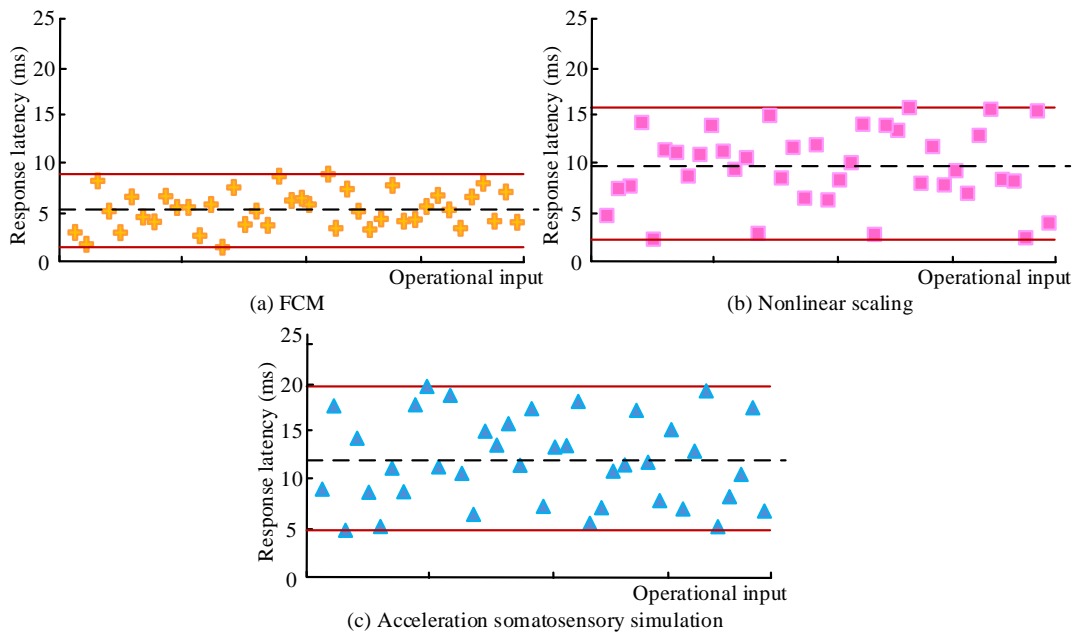


Figure 10. Device response latency

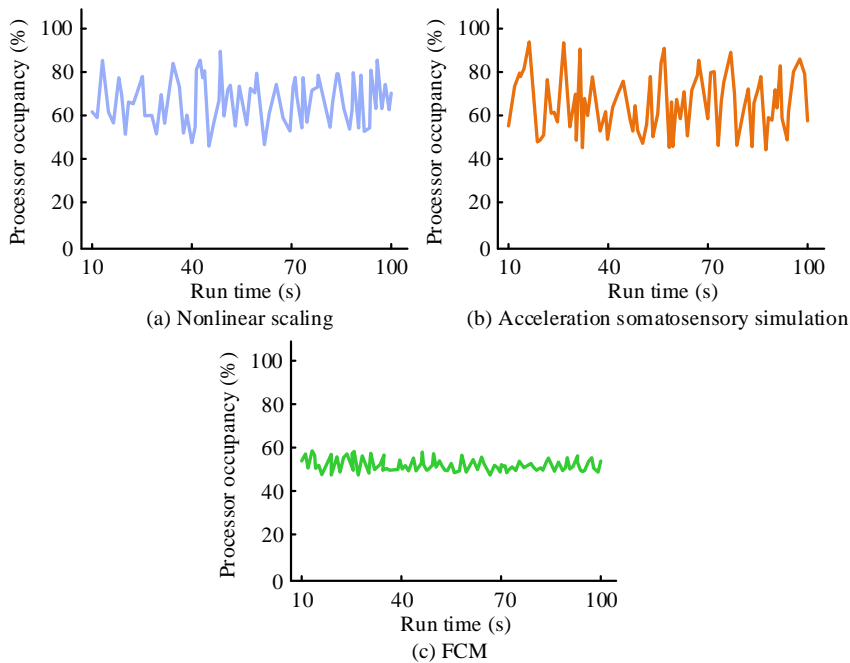


Figure 11. Processor occupancy

Fig. 11 shows that the processor usage of different methods during runtime fluctuates within a certain range. Among them, the processor occupation within the operation of the nonlinear scaling method, the acceleration body-sensing simulation method and FCM is the highest, reaching 90%, 92% and 58% respectively. This indicates that the research method has a more balanced distribution of computation at runtime and less performance consumption on hardware. Set the screen resolution to 2 K, adjust the detail level of the software screen to full height, turn on the motion blur function, and output the same simulation screen. The graphics card occupancy when the simulator is running is analyzed, as shown in Fig. 12.

From Fig. 12, it can be seen that the graphics card occupancy trend during runtime is basically the same for different methods. Among them, the nonlinear scaling method occupies the highest proportion of about 77%; The maximum occupancy of the acceleration body sensing simulation method is about 79%; FCM has a maximum occupancy of about 68%. This indicates that the research method has more stable output effect on the screen and lower hardware performance requirements for complex

screens. Energy consumption data is collected through a combination of ammeters and voltmeters to monitor the power consumption of the entire device during operation. The total energy consumption of the device when the simulator is running is analyzed, as shown in Fig. 13.

Fig. 13 shows that when the simulator runs for 60 minutes, the total energy consumption of FCM on paved and rough roads increases to approximately 2.08 kW·h and 2.63 kW·h, respectively. This indicates that the research method has a better performance of energy consumption during operation. In order to further confirm the effectiveness of the research method, 100 students with rally driving licenses were selected for application testing, including 50 as the experimental group and 50 as the control group. The experimental group and the control group were further divided into 5 groups. The control group adopted the conventional teaching method and modified 30% of the conventional teaching time to the acceleration simulation method, while the experimental group modified 30% of the teaching time to VR digital teaching using the research method. The comparison of actual learning outcomes is shown in Table 1.

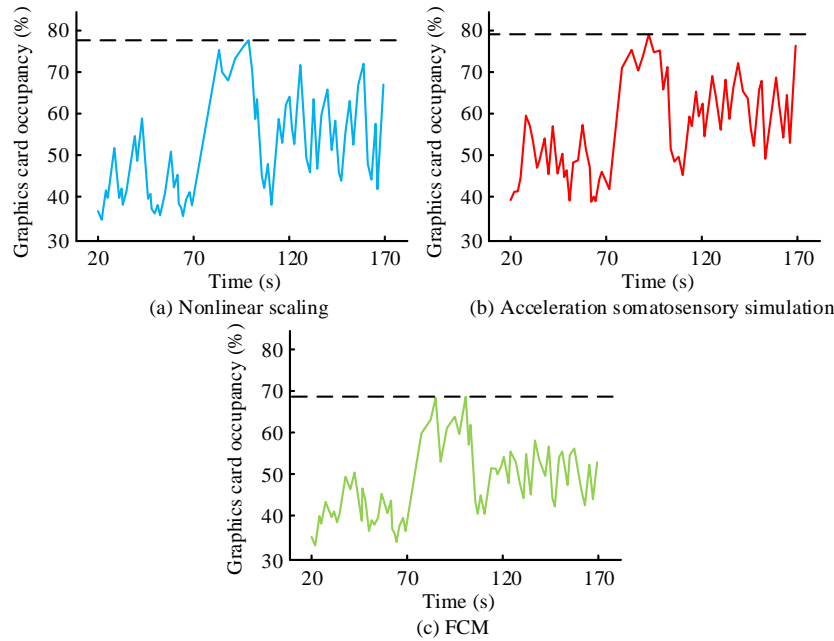


Figure 12. Graphics card occupancy

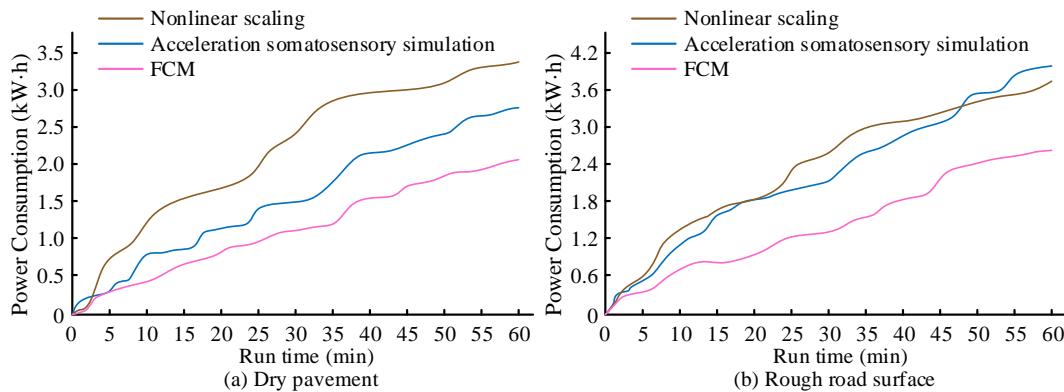


Figure 13. Total energy consumption curve of equipment operation

Table 1. Actual learning effectiveness

Group	Experimental group pass rate (%)	Control group pass rate (%)
A	70%	60%
B	60%	60%
C	70%	50%
D	70%	60%
E	70%	40%

As shown in Table 1, in actual teaching, the passing rate of the driving license exam for the five control groups remained between 40% and 60%, with three groups reaching 60%. The passing rate of the driving test for the five groups in the experimental group remained between 60% and 70%, with four groups reaching 70%. The experimental group of students used a virtual reality digital driving simulator combined with fuzzy compensation optimization elution algorithm, which improves the realism and interaction of the simulator. The fuzzy compensation technology can adjust the acceleration and G-force changes of the simulator in real time to help students better cope with different driving situations. The elution algorithm simulates the human body's perception of acceleration force, which makes the driving experience more realistic. In addition, VR technology provides an immersive learning environment that can simulate complex road conditions and emergency situations without risk, helping students improve their driving proficiency and ability to cope with stress. Therefore, students in the experimental group performed better on the driving test, while the control group did not get the same practical experience due to the limitations of traditional teaching methods. To quantitatively evaluate the effect of fuzzy compensation optimizer on improving the control accuracy of motion platforms, the performance of three algorithms was compared, including research methods, nonlinear scaling methods, and acceleration somatosensory simulation methods. The study recorded the error between the output of the platform and the expected instruction when executing the same simulation instruction, and the results are shown in Table 2.

Table 2. Performance comparison of different methods

Evaluation metric	Yest conditions	Research methodology	Nonlinear scaling	Acceleration simulation
Average position error (mm)	Dry pavement	3.2	5.8	7.1
	Rough road surface	8.5	14.3	18.9
Average attitude error (degrees)	Dry pavement	0.45	0.82	1.05
	Rough road surface	1.12	1.97	2.54
Peak load of processor (%)	Run for 100 seconds	58	90	92
Energy consumption (kilowatt hours)	60 minute run	2.08	3.41	2.75

According to Table 2, the research method consistently outperforms the comparative algorithms in all key

indicators. The significant reduction in average position and attitude errors indicates that the fuzzy compensation mechanism effectively optimizes the parameters of the washout algorithm, thereby achieving more precise control of the motion platform and more accurate reproduction of the target motion prompt. In addition, the lower peak load and energy consumption of the processor indicate that the research method achieves higher fidelity motion cues without incurring additional computational or energy overhead, highlighting its efficiency. These results validate the effectiveness of the fuzzy rule library based on empirical design in improving the performance of driving simulator systems.

5. DISCUSSION

5.1. Summary and Discussion

The experimental results comprehensively demonstrate that the FCM method proposed in the study has superior performance in calculating load, reliability, and energy consumption. In terms of computational efficiency, the peak processor occupancy rate of FCM during runtime is only 58%, significantly lower than the requirements of traditional nonlinear scaling methods (90%) and acceleration body sensing simulation methods (92%). This is because of the efficiency of fuzzy reasoning mechanisms, which dynamically adjust parameters through simple rule evaluation rather than relying on computationally intensive online optimization or fixed, overly conservative scaling strategies. Therefore, lower processing requirements directly translate into higher system energy efficiency. In the 60 minute simulation, the total energy consumption of FCM on paved roads was only 2.08 kW · h, which was reduced by about 39% and 24% compared to the two benchmark methods, respectively. In addition to efficiency, FCM also exhibits significantly improved operational reliability and stability. It achieves lower and more consistent device response latency, averaging 5.3 ms with fluctuations ranging from 1.3ms to 8.9 ms. This reduced and predictable delay is crucial for minimizing the time difference between motion cues and visual feedback, effectively alleviating the risk of perceptual conflicts and related simulator vertigo, which in turn supports the robustness and reliability of the system in long-term, dynamic driving scenarios. In summary, the collaborative integration of washout algorithms and fuzzy compensation not only performs excellently in improving motion realism, but also imposes lighter computational loads, ensures higher operational stability, and consumes less energy while achieving this goal, providing a more sustainable and high-performance solution for VR based driving simulators.

5.2. Future Work

In future research, the following improvement measures can be taken. Firstly, the current fuzzy rule base relies on mechanism analysis and expert experience. In the future, online adaptive mechanisms such as reinforcement learning will be introduced to achieve dynamic optimization and self correction of membership function parameters and rule conclusions, thereby enhancing the system's generalization ability in untrained scenarios. Secondly, this study focuses

on optimizing motion suggestion algorithms. Future work will integrate vehicle dynamics models with reference path tracking controllers, and introduce Lyapunov stability theory or frequency domain analysis methods to provide strict theoretical guarantees for the closed-loop stability of the entire simulation system. In addition, exploring the integration of multimodal sensory feedback (such as tactile and auditory) with existing motion prompt systems in order to enhance immersion in a more dimensional way is also an important research direction for the future.

6. CONCLUSION

The research designed a driving learning simulator VR digital technology based on fuzzy compensation optimization of washout algorithm to improve the quality of automobile driving technology training. In the process, the simulator motion model including moving platform and static platform is designed, the transfer function of motion information is constructed, and the motion control of the simulator is realized through the angular and distance signals, and then the fuzzy controller is inserted into the washout algorithm to realize the fuzzy compensation, and the general form of the fuzzy is represented using the affiliation function, and the structure of the washout algorithm is reconstructed, and the driving learning simulation technology realization process is designed by the VR equipment cooperating with the simulator, and the VR equipment cooperating with the simulator is designed. The implementation process of driving learning simulation technology by VR equipment with simulator is designed, and finally the effectiveness of the research method is analyzed. By dynamically optimizing the filtering parameters and gain weights, the fuzzy compensation technology effectively reduces the platform reset delay and perceptual distortion, and decreases the sensory conflict between the visual and vestibular systems, thereby significantly alleviating simulator sickness. Experimental data show that the average response delay of the device is only 5.3 ms, and the maximum processor occupancy rate is only 58%. This indicates that the real-time performance and stability of the system can effectively suppress the asynchronous problem of motion signals and visual feedback, further reducing the discomfort of users. The experimental results show that in the output position error test, the output position error of the research method is 7.7mm when the instantaneous G-force reaches 1.3 in the paved road; in the equipment response delay test, the response delay of the equipment operation of the research method fluctuates from 1.3 ms to 8.9 ms; when analyzing the graphic card occupancy, the highest graphic card occupancy of the research method is 68%; the research method runs for 60 min in the paved road environment. The total energy consumption of the research method is only 2.08 kW-h for 60 min of operation in a paved road environment, indicating that the research method has a higher accuracy of data output and is able to complete the driving simulation with lower hardware and energy requirements. However, current research has only designed specialized methods for 4-wheeled vehicles, and the adaptation and optimization of special vehicles such as 2-wheeled and 6-wheeled vehicles are not yet perfect. In the future, we can try to analyze the characteristics of vehicles

with different numbers of wheels and driving types to optimize the method in detail, expand the applicability of the method without excessively expanding the algorithm volume, and provide technical assistance for teaching special vehicle driving techniques. In addition, it is possible to explore the combination of research methods with vehicle dynamics models, and introduce rule-based self optimization mechanisms based on reinforcement learning and rigorous stability theory analysis to construct a more comprehensive driving simulation control system.

Funding Declaration

No Funding.

Data Availability declaration

The datasets used and/or analysed during the current study available from the corresponding author on reasonable request.

Competing Interest declaration

The authors have declared that no competing interests exist.

Author Contribution declaration

S.W. writing—original draft; formal analysis. B.C. methodology; writing—review & editing.

References

- [1] J. D. Lee, S. Y. Liu, J. Domeyer, A. DinparastDjadid, "Assessing drivers' trust of automated vehicle driving styles with a two-part mixed model of intervention tendency and magnitude", *Human Factors*, Vol. 63, No. 2, 2021, pp.197-209. <https://doi.org/10.1177/0018720819880363>.
- [2] É. Zablocki, H. Ben-Younes, P. Pérez, M. Cord, "Explainability of deep vision-based autonomous driving systems: Review and challenges", *International Journal of Computer Vision*, Vol. 130, No. 10, 2022, pp.2425-2452. <https://doi.org/10.1007/s11263-022-01657-x>.
- [3] Z. Gao, X. Yan, F. Gao, L. He, "Driver-like decision-making method for vehicle longitudinal autonomous driving based on deep reinforcement learning", *Proceedings of the Institution of Mechanical Engineers, Part D: Journal of Automobile Engineering*, Vol. 236, No. 13, 2022, pp.3060-3070. <https://doi.org/10.1177/09544070211063081>.
- [4] Y. Huang, K. M. Kockelman, V. Garikapati, L. Zhu, S. Young, "Use of shared automated vehicles for first-mile last-mile service: micro-simulation of rail-transit connections in Austin, Texas", *Transportation Research Record*, Vol. 2675, No. 2, 2021, pp.135-149. <https://doi.org/10.1177/0361198120962491>.
- [5] L. Garber, S. Khodaei, Z. Keshavarz-Motamed, "The critical role of lumped parameter models in patient-specific cardiovascular simulations", *Archives of Computational Methods in Engineering*, Vol. 29, No. 5, 2022, pp.2977-3000. <https://doi.org/10.1007/s11831-021-09685-5>.
- [6] H. Azevedo-Sa, S. K. Jayaraman, C. T. Esterwood, X. J. Yang, L. P. Robert Jr, D. M. Tilbury, "Real-time estimation of drivers' trust in automated driving systems", *International Journal of Social Robotics*, Vol. 13, No. 8, 2021, pp.1911-1927. <https://doi.org/10.1007/s12369-020-00694-1>.

- [7] C. Zhai, C. Chen, X. Yang, G. Liu, C. Yan, F. Luo, J. Xu, "Ecological driving for connected and automated vehicles at unsaturated intersections considering queue effects", *IEEE Transactions on Vehicular Technology*, Vol. 71, No. 12, 2022, pp.12552-12563. <https://doi.org/10.1109/TVT.2022.3199562>.
- [8] H. Liu, Y. Tian, J. Sun, D. Wang, "An exploration of data-driven microscopic simulation for traffic system and case study of freeway", *Transportmetrica B: Transport Dynamics*, Vol. 11, No. 1, 2023, pp.301-324. <https://doi.org/10.1080/21680566.2022.2064361>.
- [9] I. Miri, A. Fotouhi, N. Ewin, "Electric vehicle energy consumption modelling and estimation-A case study", *International Journal of Energy Research*, Vol. 45, No. 1, 2021, pp.501-520. <https://doi.org/10.1002/er.5700>.
- [10] Y. Ding, W. Zhuang, L. Wang, J. Liu, L. Guvenc, Z. Li, "Safe and optimal lane-change path planning for automated driving", *Proceedings of the Institution of Mechanical Engineers, Part D: Journal of Automobile Engineering*, Vol. 235, No. 4, 2021, pp.1070-1083. <https://doi.org/10.1177/0954407020913735>.
- [11] Z. Wu, L. Zhao, G. Liu, J. Chai, J. Huang, X. Ai, "The effect of AR-HUD takeover assistance types on driver situation awareness in highly automated driving: A 360-degree panorama experiment", *International Journal of Human-Computer Interaction*, Vol. 40, No. 20, 2024, pp.6492-6509. <https://doi.org/10.1080/10447318.2023.2254645>.
- [12] L. H. R. H. Zeuwts, R. Vanhuele, P. Vansteenkiste, F. J. Deconinck, M. Lenoir, "Using an immersive virtual reality bicycle simulator to evaluate hazard detection and anticipation of overt and covert traffic situations in young bicyclists", *Virtual Reality*, Vol. 27, No. 2, 2023, pp.1507-1527. <https://doi.org/10.1007/s10055-023-00746-7>.
- [13] H. Zhang, L. Cao, G. Howell, D. Schwartz, C. Peng, "An educational virtual reality game for learning historical events", *Virtual Reality*, Vol. 27, No. 4, 2023, pp.2895-2909. <https://doi.org/10.1007/s10055-023-00845-5>.
- [14] T. Houda, L. Beji, A. Amouri, M. Mallem, "Handiski simulator performance under PSO-based washout and control parameters optimization", *Nonlinear Dynamics*, Vol. 110, No. 1, 2022, pp.649-667. <https://doi.org/10.1007/s11071-022-07626-w>.
- [15] P. Duc-An, N. Duc-Toan, "A novel motion cueing algorithm integrated multi-sensory system-Vestibular and proprioceptive system", *Proceedings of the Institution of Mechanical Engineers, Part K: Journal of Multi-body Dynamics*, Vol. 234, No. 2, 2020, pp.256-271. <https://doi.org/10.1177/1464419319895351>.
- [16] B. Kalyanaraman, M. H. Meylan, B. Lamichhane, "Coupled Brinkman and Kozeny-Carman model for railway ballast washout using the finite element method", *Journal of the Royal Society of New Zealand*, Vol. 51, No. 2, 2021, pp.375-388. <https://doi.org/10.1080/03036758.2020.1789678>.
- [17] M. R. C. Qazani, H. Asadi, S. Nahavandi, "A motion cueing algorithm based on model predictive control using terminal conditions in urban driving scenario", *IEEE Systems Journal*, Vol. 15, No. 1, 2020, pp.445-453. <https://doi.org/10.1109/JSYST.2020.2994154>.
- [18] B. Dasu, S. Mangipudi, S. Rayapudi, "Small signal stability enhancement of a large scale power system using a bio-inspired whale optimization algorithm", *Protection and Control of Modern Power Systems*, Vol. 6, No. 1, 2021, pp.1-17. <https://doi.org/10.1186/s41601-021-00215-w>.
- [19] C. Savaglio, G. Fortino, "A simulation-driven methodology for IoT data mining based on edge computing", *ACM Transactions on Internet Technology (TOIT)*, Vol. 21, No. 2, 2021, pp.1-22. <https://doi.org/10.1145/3402444>.
- [20] H. Yokus, A. Ozturk, "A robust crow search algorithm-based power system stabilizer for the SMIB system", *Neural Computing and Applications*, Vol. 34, No. 11, 2022, pp.9161-9173. <https://doi.org/10.1007/s00521-022-06943-w>.
- [21] A. Wellendorf, P. Tichelmann, J. Uhl, "Performance analysis of a dynamic test bench based on a linear direct drive", *Archives of Advanced Engineering Science*, Vol. 1, No. 1, 2023, pp.55-62. <https://doi.org/10.47852/bonviewAAES3202902>.
- [22] A. Hameed, A. S. S. Abadi, A. Ordys, "Model predictive control based motion cueing algorithm for driving simulator", *Journal of Systems Science and Systems Engineering*, Vol. 33, No. 5, 2024, pp.607-626. <https://doi.org/10.1007/s11518-023-5584-6>.
- [23] A. I. M. Almadi, R. E. Al Mamlook, Y. Almarhabi, I. Ullah, A. Jamal, N. Bandara, "A fuzzy-logic approach based on driver decision-making behavior modeling and simulation", *Sustainability*, Vol. 14, No. 14, 2022, p.8874. <https://doi.org/10.3390/su14148874>.
- [24] H. B. Moussa, M. Bakhti, "Nonlinear tyre model-based sliding mode observer for vehicle state estimation", *International Journal of Dynamics and Control*, Vol. 12, No. 8, 2024, pp.2944-2957. <https://doi.org/10.1007/s40435-024-01383-x>.
- [25] M. Bruschetta, K. N. D. Winkel, E. Mion, P. Pretto, A. Beghi, H. H. Bülthoff, "Assessing the contribution of active somatosensory stimulation to self-acceleration perception in dynamic driving simulators Assessing the contribution of active somatosensory stimulation to self-acceleration perception", *PLoS ONE*, Vol. 16, No. 11, 2021, e0259015. <https://doi.org/10.1371/journal.pone.0259015>.
- [26] N. Shah, A. W. Zehri, U. N. Saraih, N. A. A. Abdelwahed, B. A. Soomro, "The role of digital technology and digital innovation towards firm performance in a digital economy", *Kybernetes*, Vol. 53, No. 2, 2024, pp.620-644. <https://doi.org/10.1108/K-01-2023-0124>.
- [27] Hilda, Yulia, G. G. P, "Analysis of the utilization of digital technology for Msme in the city of Pontianak – Indonesia", *Malaysian E Commerce Journal*, Vol. 6, No. 1, 2022, pp.17-19. <https://doi.org/10.26480/mecj.01.2022.17.19>.
- [28] T. Albrecht, M. S. Baier, H. Gimpel, S. Meierhöfer, M. Röglinger, J. Schlüchtermann, L. Will, "Leveraging digital technologies in Logistics 4.0: Insights on affordances from intralogistics processes", *Information Systems Frontiers*, Vol. 26, No. 2, 2024, pp.755-774. <https://doi.org/10.1007/s10796-023-10394-6>.